Hindawi
Advances in Civil Engineering
Volume 2023, Article ID 3276832, 12 pages
https://doi.org/10.1155/2023/3276832

*Research Article*

# Numerical Simulation Study on Influence of a Structural Parameter of D Bolt, an Energy-Absorbing Rock Bolt, on its Stress Distribution

**Kwang Nam Pyon**,[1] **Kyong Su Son**,[1] **and Un Chol Han**[2]

[1]*Faculty of Mining Engineering, Kim Chaek University of Technology, Pyongyang, Democratic People's Republic of Korea*
[2]*School of Science and Engineering, Kim Chaek University of Technology, Pyongyang 999093, Democratic People's Republic of Korea*

Correspondence should be addressed to Un Chol Han; huch8272@star-co.net.kp

Received 1 February 2023; Revised 16 May 2023; Accepted 24 May 2023; Published 12 June 2023

Academic Editor: Huseyin Bilgin



A D bolt, an energy-absorbing rock bolt, is a smooth steel bar with a number of anchors along its length. The anchors, which can be spaced evenly or unevenly along its length, are firmly fixed within a borehole using either cement grout or resin, while the smooth sections of the bolt between the anchors may freely deform in response to rock dilation. A series of numerical simulations have been conducted using the finite difference method to investigate the effects of D bolt on the displacement increase of rock mass around a roadway in comparison with normal fully encapsulated rebar. As a result, the displacement of 49 mm at the top of roadway roof in the D bolts supported model is much larger than 30.08 mm in the fully encapsulated rebar bolts supported model so that the former is capable of absorbing potential deformation energy of rock mass around a roadway to tolerate the large deformation of rock. Plans of spacing arrangement of D bolt's anchor have a significant effect on stress redistribution of the bolt. The numerical simulation result shows that for the D bolt with its whole length of 2.4 m, the length of its exposed section of 0.1 m, and the 4 anchors with the length of 0.1 m, the maximum tensile stress of 3.25 GPa generated in the D bolt with the ratio of the spacing between anchors (RSA) of 30 : 40 : 50 : 70 is lower about 1.13–1.31 times than the other D bolts with different ratio of spacing, and the changing range of stress is also the smallest, where the ratio of 30 : 40 : 50 : 70 indicates a ratio of lengths of deformable sections which is determined by turns from the innermost section of rock mass around roadway to the outermost section of roadway space. This study demonstrates that it is reasonable to employ the RSA of D bolt which makes it bring out its energy-absorbing capability to the full.

## 1. Introduction

An important problem arising in underground excavation is stabilising the country rock that surrounds openings at depth. An increase in the in situ rock stresses is the essential difference between rock at depth and rock near the surface. As a consequence of such an increase in the ground, stress rock burst may be of common occurrence in hard rocks, or large squeezing deformations may appear in soft and weak rocks. It has been detected in lots of mines that such phenomena begin to occur at the depth of about 600–800 m below the surface level and become more significant below 1000 m. In many metal mines, for example, those in Sweden, Canada, West Australia, and South Africa, mining operations are currently commenced at the depth of below 1000 m and even down to 3000 m. At these depths, conventional support devices [1] may not be adapted for severe rock conditions.

Over the years, many researchers have tried to develop various ground support techniques and products for support and retention of the newly exposed faces and internal reinforcement of the soil and rock masses surrounding the excavations. Nevertheless, one can classify the rock supports into three types by their performance [2], i.e., a strength bolt,

a ductile bolt, and an energy-absorbing bolt. Moreover, recently, researches on modelling load-displacement performances of different cable bolts and assessing their mechanical performances have been also carried out [3, 4], of which application tends to increase in both underground mining operations and civil tunnel excavations.

Strength bolts can be defined as those that support a load equal to or approximate to the intrinsic strength of the bolt material. A fully encapsulated rebar bolt belongs to this category. It has a considerable load-bearing capacity; however, rebar cannot stand against large rock dilations. A fully encapsulated rebar bolt can only withstand a deformation of 2–3 cm when they are subjected to a fracture opening. The main reason why we use rebar bolts is that they can support unstable blocks fully so as to prevent rock falls. This is valid in shallow locations, which have low in situ rock stresses and the main risk from gravitational rock falls. When a fully encapsulated rebar bolt is used in weak and soft rocks or at depths, it can be frequently observed that either the face plate of the rebar is heavily loaded or the thread of the bolt is pulled out to destroy [5]. It can be known that the rebar is too stiff to undergo rock dilations in the rock masses with high stress from premature failure of the rebar bolts.

Ductile bolts are in essence plastic ones with low stiffness which is capable of being proof against large rock deformation, such as the split sets [6]. Split sets have been used as reinforcements in lots of deep mines in Australia in order to undergo rock dilations. Although split sets are indeed capable of undergoing large rock deformations, they suffer from fairly low load-bearing capacity. Both rebar and split sets are low-energy-absorbing devices. Load-bearing capacities of several new yielding and inflatable rock bolts under axial and shear loadings have been experimentally investigated to provide a benchmark for comparison with other existing friction and yielding bolts [7].

Energy-absorbing bolts are characterized by their high load capacity and also their large deformation capacity. In the early 1990s, it was noticed that support devices used in deep mines should be able to carry high loads and also accommodate large deformations; that is, they should be capable of absorbing a large amount of energy prior to failure [8]. Various energy-absorbing bolts that can meet the mentioned requirement were developed in recent decades, such as the Garford solid dynamic bolt [9]; Roffex [10, 11]; energy-absorbing rock bolt [12]; cone bolt [13, 14]; MCB cone bolt (modified cone bolt with elongation as much as 180 mm) [15, 16]; D bolt with large load-bearing and deformation (elongation as long as 400 mm) [2]; and He bolt [17].

The D bolt is a new energy-absorbing support device developed in 2006. It is made of a smooth steel bar that has a number of integrated anchors which are spaced evenly or unevenly along its length. The difference between this bolt and other energy-absorbing bolts is that it is multipoint anchored in a fully grouted borehole. All other energy-absorbing bolts are two-point anchored in boreholes. The multipoint anchoring mechanism in the D bolt is very reliable. Failure of one section (or one anchor) will not negatively influence the rock reinforcement of the other sections of the bolt [2]. The anchors of the D bolt can be spaced evenly or unevenly along its length. It seems that plans of spacing arrangement of D bolt's anchors, one significant structural parameter of it, influence its stress distribution and stress redistribution around a roadway supported with it.

Underground excavation in a stressed rock mass induces stress redistribution of rock mass around the roadway, and depending on the geometry of the roadway, the in situ state of stress existing before the roadway is excavated on the material properties as well as the pattern and capacity of the roadway support [18]. For the roadway stability, investigating these stress redistribution characteristics is very essential. Numerical simulation looks like the most suitable approach to study these issues, and many studies have been conducted using this approach [19]. A parametric study has been accomplished using the numerical analysis code FLAC3D to consider the influence of various shapes of underground openings on the maximum induced boundary stress [20]. The effects of rock bolting on the stress redistribution of rock mass around the openings have been examined by using the ANSYS software. It has been verified that rock bolting can significantly reduce both the intensity and the size of the region of stress concentration [21]. Du used the numerical analysis code FLAC3D that has been used to analyze the effects of rock bolts which are installed on different sides of a roadway and three bolting parameters including bolt spacing, length, and pretensioned force on stress redistribution around a roadway, and the ground arch action caused by rock bolting has been effectively simulated [22]. The effect of bolt inclination on the shear strength of rock joints has been analyzed by using a numerical simulation method [23].

Most of the previous studies have proposed numerical simulation methods of fully encapsulated rebar bolt and analyzed its action effects. In the present study, we carry out a numerical simulation of D bolt, a type of energy-absorbing rock bolt which is not fully encapsulated but multipoint anchored in a fully grouted borehole. Then, the influence of the spacing arrangement of its anchors on its axial stress distribution is discussed, and the rational plan is selected.

The aim of this study is to verify the energy-absorbing effect of D bolt in comparison with a fully encapsulated rebar bolt and to select a rational plan of spacing arrangement of its anchors so that its deformable sections could be more evenly loaded, which can prevent the premature failure of steel bar and improve load-bearing and deformation capacity of D bolt to provide sufficient support to high-stress rock mass.

## 2. Numerical Simulation Methodology and Input Parameters

This study has used FLAC3D numerical analysis code developed by ITASCA Consulting Group. The basis of this code is the finite difference numerical method with the Lagrangian calculation method. The finite difference method (FDM) can be more effectively applied to modelling of stress distribution around an underground roadway in comparison with other numerical techniques [24].

*2.1. Model Generation.* A geometric model has been generated as a plane strain model for present numerical analysis studies by using a radial cylinder grid and radial tunnel grid, as shown in Figure 1. The length, width, and height of the geometric model are 60 m, 1 m, and 60 m, respectively. An arch roadway is placed in the center of the model. Its width and linear wall height are 4 m and 1.5 m, and radius and height of the arch are 2 m and 2 m, respectively. The typical element size in the region near to the roadway is approximately 0.2 m × 0.04 m × 0.1 m.

The model is single material. The strain-softening constitutive model has been employed to present the stress-strain behavior of the rock material. The input parameters of rock material for the model include density, elastic modulus, Poisson's ratio, bulk modulus, shear modulus, cohesion, friction angle, and tensile strength of rock mass surrounding the roadway. The mechanical properties of the rock specimen were obtained from the laboratory test using an MTS C60 hydraulic servo-control testing machine, based on the ISRM suggested method, and the parameters of rock mass were estimated using the RocLab software. The material properties are listed in Table 1.

The model is constructed as plates of unit thickness, with a boundary condition of zero displacement applied on both faces. The vertical displacements at the bottom and at the top of the model are both fixed. The horizontal stresses in both directions and the vertical stress have been assumed to have the same magnitude, 18.7 MPa. Only the weight of the rock itself in the model acts on rock mass around the roadway.

*2.2. Methodology of D Bolting Simulation.* When used in FLAC3D, the structure element called "Cable" is often used to model rock bolts. The deformable section length of a D bolt is modeled by setting two parameters of the cable element, the grout stiffness per unit length and the grout shear strength per unit length, to values near to zero, and each anchor length of it is set the values of these two parameters of the cable element with the length corresponding to an anchor at a given location. The number of anchors is 4, their lengths are 0.1 m, respectively, and the exposed section of the bolt has a length of 0.1 m. Thus, the effective deformable length of the bolt would be approximately 1.9 m, excluding the total length of the anchors and the length of the exposed section. The bearing plate, which is a component of the rock bolting system, is modeled by creating a rigid node-to-zone connection between the head node of the cable element and the zone element closest to the node. The pretensioned force of the rock bolt is not applied in particular.

The rock bolts are installed in five different directions in the cross section of a roadway. The input parameters of rock bolts and grout for the model were obtained from the in-situ pullout tests in rock [25], which are given in Table 1.

## 3. Numerical Results and Discussion

*3.1. General Effects of D Bolt on Displacement of a Roadway and Stress Distribution of Rock Bolt.* When supported on a roadway in high-stress rock masses by D bolts, their action

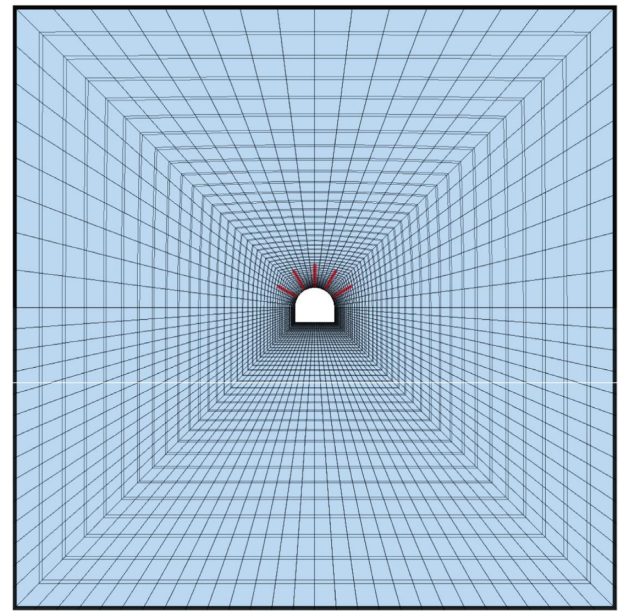


Figure 1: Numerical analysis model geometry.

effects can be accessed by comparing displacements of points on the roadway contour and stress distribution of rock bolts obtained from the models among which the fully encapsulated rebar bolt and D bolts supported, respectively. In this section, we discuss the analytic results of the models supported by the fully encapsulated rebar and D bolt that has a number of integrated anchors spaced evenly with interval of 0.475 m along its length, respectively. Figures 2–4, respectively, show the history curve of displacement at the top of the roadway roof, the stress redistribution around the roadway, and the stress distribution of rock bolts obtained from the fully encapsulated rebar bolt supported model. In all figures of this paper, units of stress and displacement are Pa and *m*, respectively.

Figures 5–7, respectively, show the history curve of displacement at the top of the roadway roof and the stress states of rock masses around the roadway and rock bolts obtained from the D bolts supported model.

The stress distributions of each bolt in two models which fully encapsulated rebar bolt supported and D bolts with anchors spaced evenly are listed in Table 2. In Table 2, positive values indicate tensile stress and negative values indicate compressive stress.

Comparison of Figures 2 and 5 shows that the displacement of 49 mm at the top of roadway roof in the D bolts supported model is relatively larger than 30.08 mm in the fully encapsulated rebar bolts supported model. As shown in Figures 4 and 7 and Table 2, the maximum axial tensile stress generated in bolts of the fully encapsulated rebar bolts supported model is 33 GPa, which is about 10 times larger than 3.4 MPa of the D bolts supported model. The above

Table 1: Input parameters for ground and D bolt.

| Input parameters | Parameters | Values |
|---|---|---|
| For ground | Density (kg/m$^3$) | 2390 |
| | Elastic modulus (GPa) | 11.1 |
| | Poissons' ratio $\nu$ | 0.29 |
| | Bulk modulus (GPa) | 8.8 |
| | Shear modulus (GPa) | 4.3 |
| | Cohesion $c$ (MPa) | 3.84 |
| | Friction angle $\varphi$ (°) | 14.4 |
| | Tensile strength (MPa) | 8.0 |
| For D bolt | Length (m) | 2.4 |
| | Density (kg/m$^3$) | 7850 |
| | Elastic modulus (MPa) | $2.0 \times 10^5$ |
| | Tensile yield strength (MPa) | 240 |
| | Cross-sectional area(m$^2$) | $2 \times 10^{-4}$ |
| | Number of D bolts in a roadway cross section | 5 |
| | Number of anchors for each D bolt | 4 |
| | Length of each anchor (m) | 0.1 |
| | Grout cohesive strength per unit length for each anchor (kN/m) | 425 |
| | Grout stiffness per unit length for each anchor (kN/m) | $2 \times 10^6$ |
| | Grout friction angle (°) | 35 |

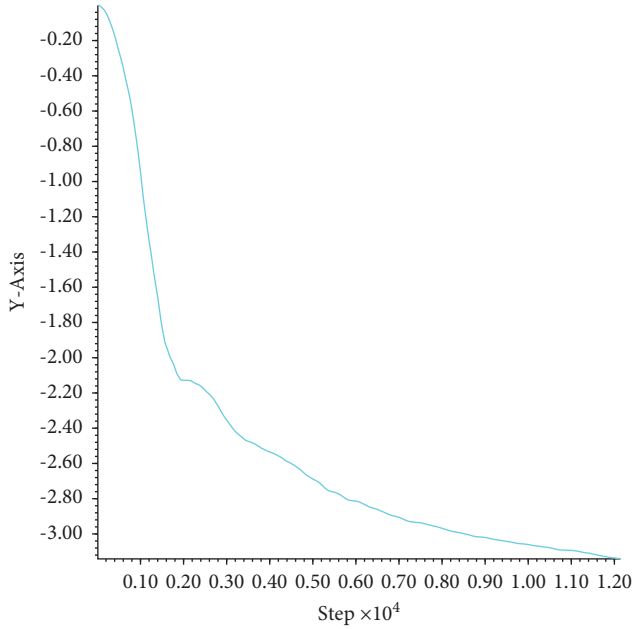


Figure 2: The history curve of displacement at the top of the roadway roof in the fully encapsulated rebar bolt supported model.

results indicate that D bolts are indeed capable of tolerating larger deformation of rock mass around a roadway than stiff rebar; that is, they have the capability of absorbing potential deformation energy of rock mass around a roadway. A comparison of the four plots in Figures 3 and 6 fails to show an obvious difference in the stress states of rock masses around the roadway. The reason is that stress changes between the two models are so small, compared with in situ stresses which have initially been applied to the models that they could not be noticeably observed in these stress contour plots.

As shown in Table 2, the displacement of roadway contour in the fully encapsulated rebar bolts supported model is smaller than those in D bolts supported model, but the force acting on rebar is much larger than D bolt, so that it can be broken. For example, the magnitudes of maximum stresses generated in the second and third segments of four rebar bolts, excluding the first bolt, are 33 GPa, exceed the yield strength of the material, so the rebar may be broken. In the D bolt supported model, however, the stress generated in the D bolt is so approximately 10 times smaller than the rebar bolt, and its stability is reliable because it tolerates displacement of rock mass around a roadway to a certain degree.

*3.2. Effects of Spacing Arrangement of D Bolt's Anchors on Stress Distribution of the Bolt.* The displacement of rock mass around a roadway depends on the distance from the contour of the roadway to the given point. Commonly, the nearer to the contour of roadway the point is, the larger the displacement of rock mass is, and the further is, the smaller is. The field tests of the D bolt show that the outermost and innermost sections of the D bolt, which had a number of integrated anchors spaced evenly and was installed in the pillar, were the most and least loaded, respectively [2]. The reason why the axial load of each deformable section of the D bolt is different is that the magnitude of displacement generated in each deformable section is not the same, which shows that the spacing arrangement of D bolt's anchors influences on stress distribution of the bolt in a certain degree.

Therefore, in this section, we consider the effects of the spacing arrangement of D bolt's anchors on the stress distribution of the bolt. For this, numerical simulations are accomplished while changing the spacing arrangement of the D bolt's anchors differently in the model whose roadway is in the high-stress rock mass and is supported by the D bolt.

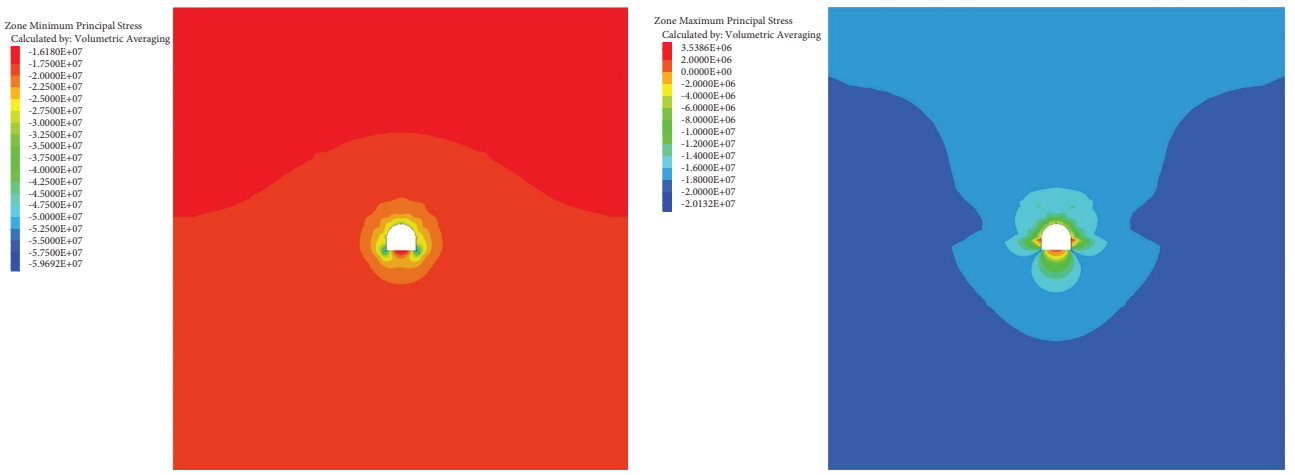


Figure 3: Stress redistribution of rock masses in the fully encapsulated rebar bolt supported model: (a) major principal stress and (b) minor principal stress.

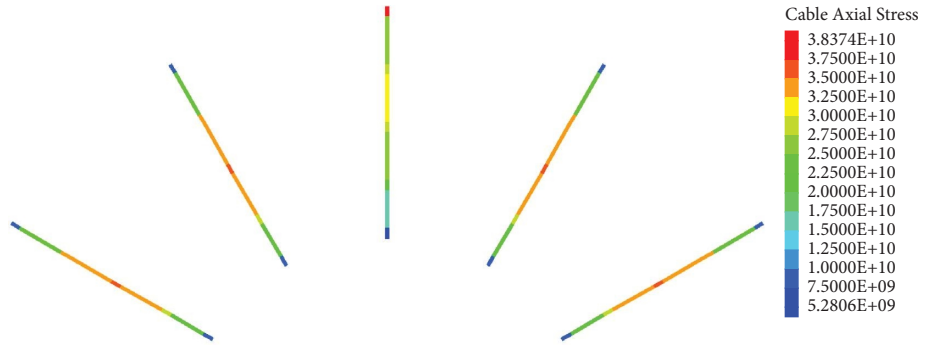


Figure 4: Stress distribution of rock bolts in the fully encapsulated rebar bolt supported model.

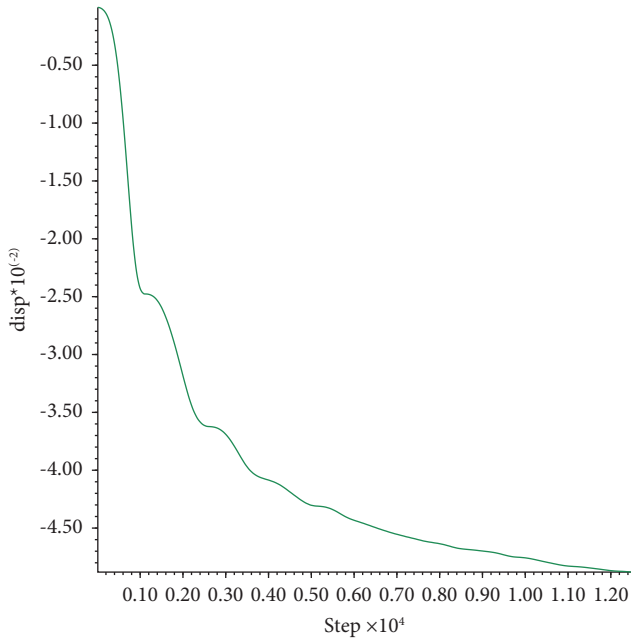


Figure 5: The history curve of displacement at the top of the roadway roof in the D bolts supported model.

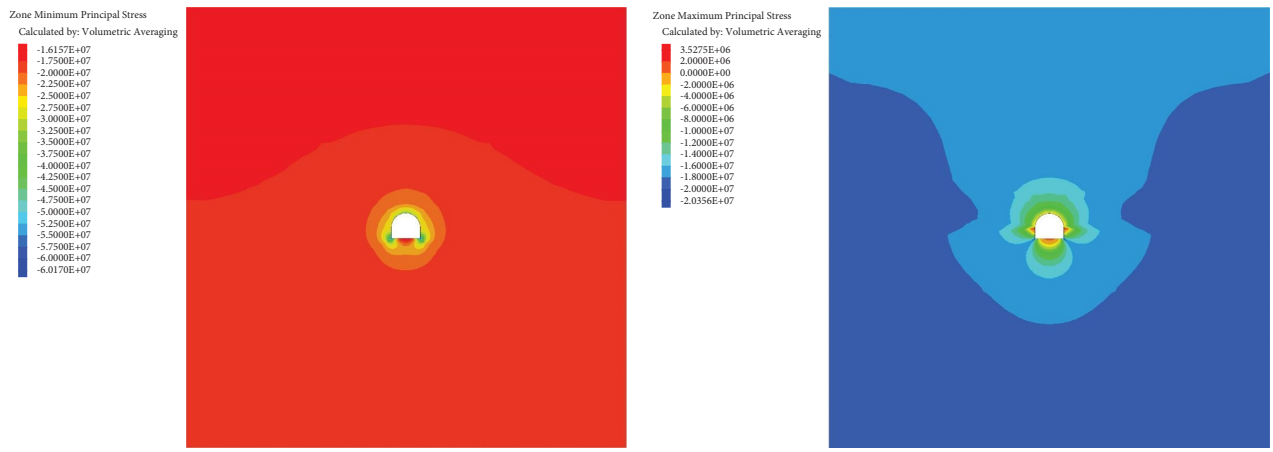


(a) (b)

FIGURE 6: Stress redistribution of rock masses in the D bolts supported model: (a) major principal stress and (b) minor principal stress.

Figures 8 and 9 show the history curves of displacement at the top of the roadway roof and axial stress distributions of the bolt obtained from the models supported by D bolts with the ratio of the spacing between anchors (RSA) of 70 : 50 : 40 : 30, 60 : 50 : 40 : 40, 40 : 40 : 50 : 60, and 30 : 40 : 50 : 70 in turns from the innermost section of rock mass around roadway to the outermost section of roadway space, respectively. In this study, a ratio of the spacing between anchors (RSA) of a D bolt means a length ratio of deformable sections in turns from the end of the bolt to its head. For example, RSA of 70 : 50 : 40 : 30 indicates that the D bolt has four deformable sections, and their lengths are, respectively, 70 cm, 50 cm, 40 cm, and 30 cm from the end of the bolt. As shown in Figure 8, the history curves of displacement at the top of the roadway roof in the models supported by D bolts with different ratios of spacing between anchors are very similar to each other, but the displacement rate at the top of the roadway roof in case of D bolt with RSA of 70 : 50 : 40 : 30 is a little larger than in the other cases.

The magnitudes of stresses generated in each segment (i.e., deformable section) of D bolts in the models supported by D bolts with different ratios of spacing among anchors are summarized in Table 3, where the ratios of spacing among anchors and numbers of segments mean length ratios and numbers of deformable sections which are determined by turns from the innermost section of rock mass around roadway to the outermost section of roadway space. In Figure 9 and Table 3, the first D bolt is one installed at the top of the roadway roof, the second and fourth bolts are those installed in the higher and lower parts of the left cross section of the roadway, respectively, and the third and fifth bolts are bolts arranged in the higher and lower parts of the right cross section of the roadway, respectively.

Figure 10 shows the magnitudes of stresses generated in the deformable sections of D bolts with different ratios of spacing among anchors comparatively, i.e., the change curves of axial stresses acting on each deformable section of five D bolts installed in different directions in the cross section of a roadway, which have RSA of 70 : 50 : 40 : 30, 60 : 50 : 40 : 40, 40 : 40 : 50 : 60, and 30 : 40 : 50 : 70, respectively. As shown in Figures 9 and 10(a)–10(e), for these five D bolts, the stress changes according to RSA are the largest at the deformable sections arranged in the outermost section of roadway space, the stress changes at the deformable sections in the innermost section of rock mass around roadway are lower than the former, and the magnitudes of stresses are very similar. For RSA of 70 : 50 : 40 : 30, the magnitude of maximum axial tensile stress generated at the deformable section arranged in the outermost section of roadway space is 4.25 GPa, which is the largest. It exceeds the tensile yield strength of bolt material, but the bolt is not broken as shown in Figure 9(a). The simulation result for RSA of 70 : 50 : 40 : 30 shows that RSA with the gradual decrease to the outermost section of roadway space is not reasonable because the displacement of surrounding rock to the contour of roadway increases; hence, the tensile load acting on D bolt also does.

Diagrams in Figure 10 show that the average stress generated in deformable sections of D bolts installed in the cross section of roadway is the smallest in the case of the bolt with RSA of 30 : 40 : 50 : 70. At this time, the magnitude of maximum tensile stress of the bolt is 3.25 GPa and is about 1.13–1.31 times smaller than other cases, and the changing range of stresses is the smallest so that it can be considered that the stress distribution along the whole length of a bolt is comparatively even. This result indicates that the application of RSA with the gradual increase to the outermost section of roadway space enables to effectively use the potential deformation and load-carrying capacity of D bolt.

*3.3. Verification of Simulation Results.* Twenty samples of D bolts with paddle anchors were field tested in a coal mine that has serious squeezing rock conditions, and they were installed with cement grout in the five different directions of the roadway section. The bolts are 16 mm in diameter and 2.4 m long and have four paddle anchors. Fifteen bolts have anchors spaced evenly, and the others' anchors are

Table 2: Axial stresses of segments in each rock bolt, Pa.

| Types of rock bolt | Number of segments | Number of bolts | | | | |
|---|---|---|---|---|---|---|
| | | № 1 | № 2 | № 3 | № 4 | № 5 |
| For fully encapsulated rebar bolt (displacement of 0.03008 m) | 1 | $1.5E+10$ | $2.25E+10$ | $2.25E+10$ | $2.25E+10$ | $2.25E+10$ |
| | 2 | $2.25E+10$ | $3.3E+10$ | $3.3E+10$ | $3.3E+10$ | $3.3E+10$ |
| | 3 | $3.1E+10$ | $3.3E+10$ | $3.3E+10$ | $3.3E+10$ | $3.3E+10$ |
| | 4 | $2.25E+10$ | $2.3E+10$ | $2.3E+10$ | $2.25E+10$ | $2.25E+10$ |
| For D bolt with anchors spaced evenly (displacement of 0.049 m) | 1 | $2.1E+09$ | $2.3E+09$ | $1.7E+09$ | $1.6E+09$ | $1.6E+09$ |
| | 2 | $3.2E+09$ | $2.8E+09$ | $2.8E+09$ | $2.7E+09$ | $2.7E+09$ |
| | 3 | $3.4E+09$ | $3.2E+09$ | $3.2E+09$ | $3.3E+09$ | $3.3E+09$ |
| | 4 | $1.8E+09$ | $2.3E+09$ | $2.3E+09$ | $2.25E+09$ | $2.25E+09$ |

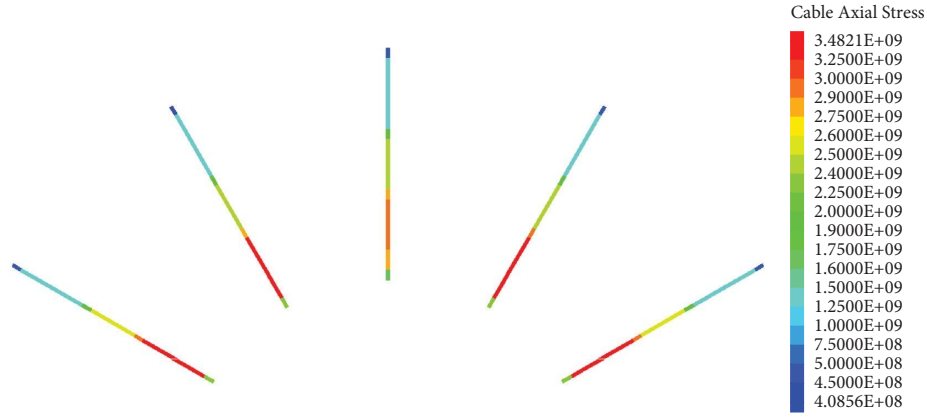


Figure 7: Stress distribution of rock bolts in the D bolts supported model.

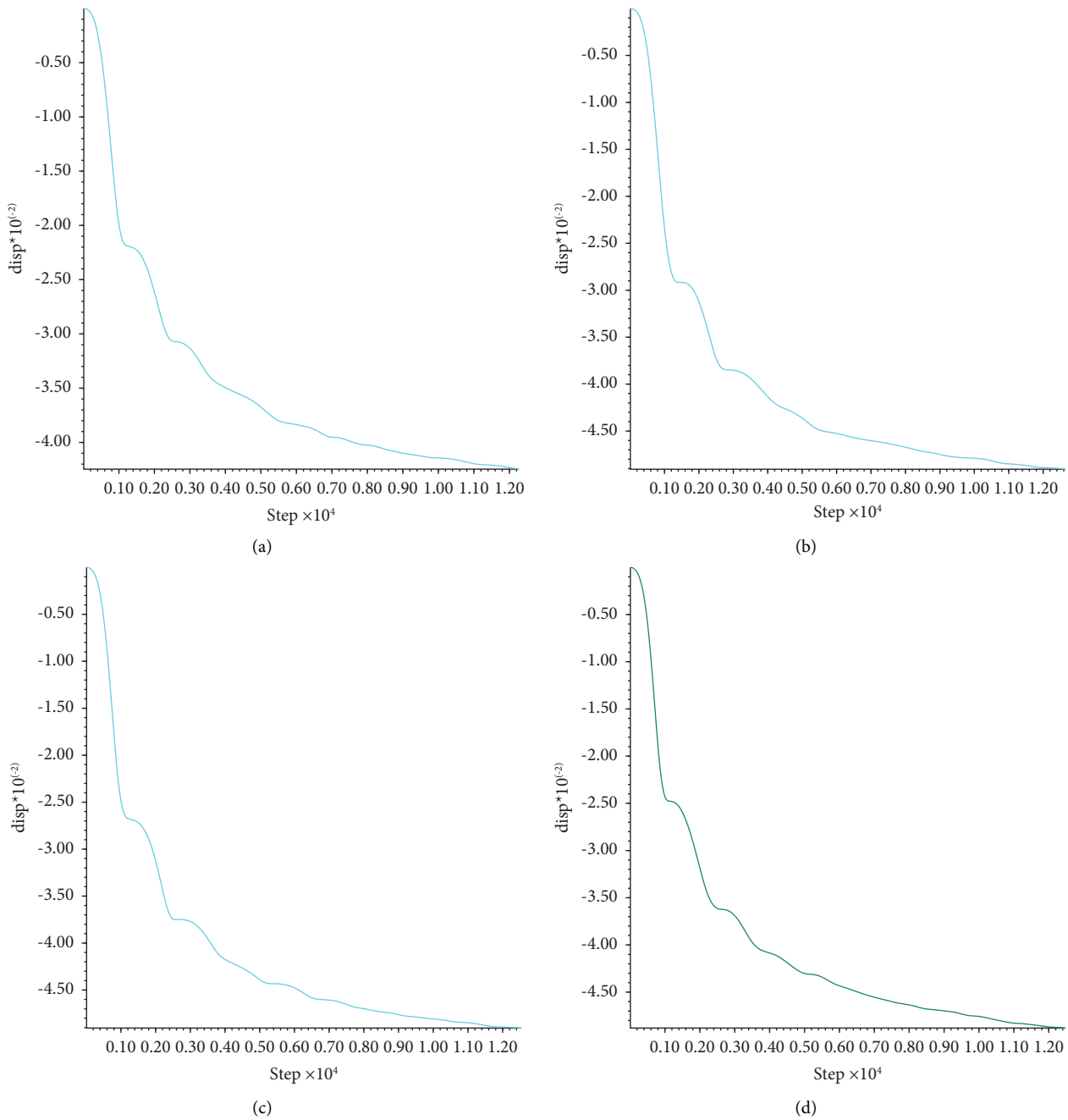


Figure 8: The history curves of displacement at the top of the roadway roof in the models supported by D bolts with RSA of (a) 70 : 50 : 40 : 30, (b) 60 : 50 : 40 : 40, (c) 40 : 40 : 50 : 60, and (d) 30 : 40 : 50 : 70.

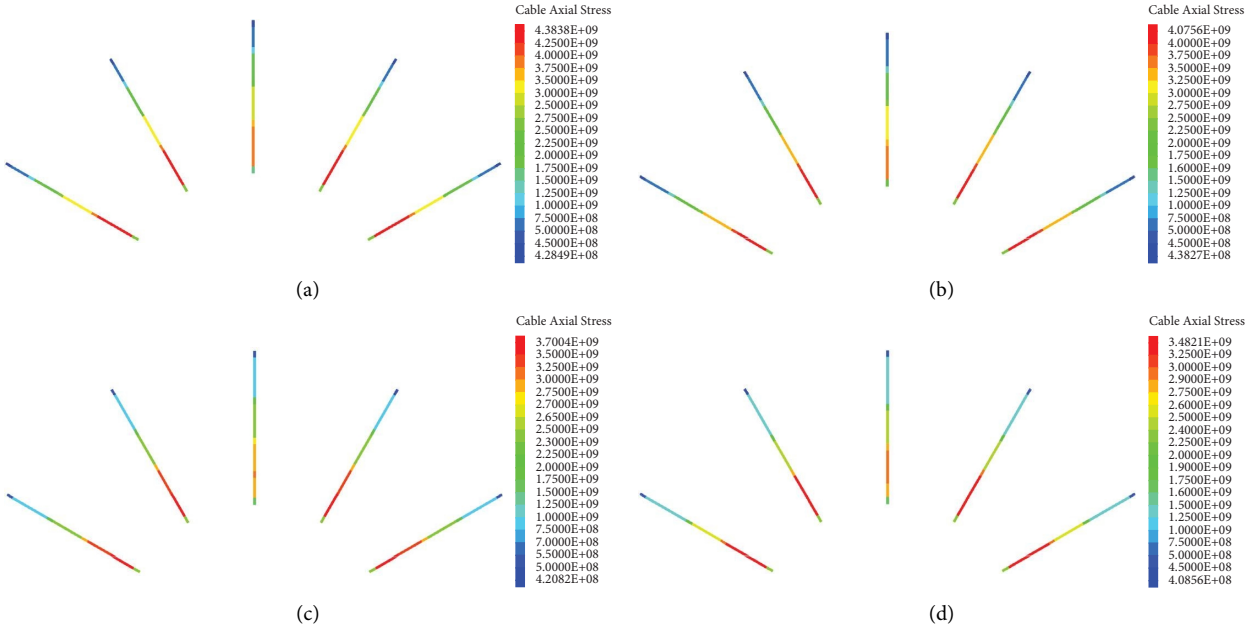


Figure 9: Axial stress distributions of bolts in the models supported by D bolts with RSA of (a) 70 : 50 : 40 : 30, (b) 60 : 50 : 40 : 40, (c) 40 : 40 : 50 : 60, and (d) 30 : 40 : 50 : 70.

Table 3: Axial stresses of segments in D bolts with different ratios of spacing among anchors, Pa.

| RSA | Number of segments | Number of D bolts | | | | |
|---|---|---|---|---|---|---|
| | | 1 | 2 | 3 | 4 | 5 |
| For 70 : 50 : 40 : 30 | 1 | $1.80E+09$ | $1.75E+09$ | $1.75E+09$ | $1.75E+09$ | $1.75E+09$ |
| | 2 | $3.10E+09$ | $3.10E+09$ | $3.10E+09$ | $3.00E+09$ | $3.00E+09$ |
| | 3 | $4.25E+09$ | $4.25E+09$ | $4.25E+09$ | $4.20E+09$ | $4.20E+09$ |
| | 4 | $4.25E+09$ | $4.10E+09$ | $4.10E+09$ | $4.00E+09$ | $4.00E+09$ |
| For 60 : 50 : 40 : 40 | 1 | $1.85E+09$ | $1.75E+09$ | $1.75E+09$ | $1.75E+09$ | $1.75E+09$ |
| | 2 | $3.30E+09$ | $3.20E+09$ | $3.20E+09$ | $3.10E+09$ | $3.10E+09$ |
| | 3 | $4.07E+09$ | $3.80E+09$ | $3.80E+09$ | $3.80E+09$ | $3.80E+09$ |
| | 4 | $3.75E+09$ | $3.25E+09$ | $3.25E+09$ | $3.15E+09$ | $3.15E+09$ |
| For 40 : 40 : 50 : 60 | 1 | $2.25E+09$ | $2.00E+09$ | $2.00E+09$ | $1.80E+09$ | $1.80E+09$ |
| | 2 | $3.70E+09$ | $3.30E+09$ | $3.30E+09$ | $3.25E+09$ | $3.25E+09$ |
| | 3 | $3.70E+09$ | $3.30E+09$ | $3.30E+09$ | $3.25E+09$ | $3.25E+09$ |
| | 4 | $2.60E+09$ | $2.30E+09$ | $2.30E+09$ | $2.20E+09$ | $2.20E+09$ |
| For 30 : 40 : 50 : 70 | 1 | $2.25E+09$ | $2.20E+09$ | $2.20E+09$ | $2.10E+09$ | $2.10E+09$ |
| | 2 | $3.25E+09$ | $3.25E+09$ | $3.25E+09$ | $3.20E+09$ | $3.20E+09$ |
| | 3 | $3.25E+09$ | $3.00E+09$ | $3.00E+09$ | $3.00E+09$ | $3.00E+09$ |
| | 4 | $2.25E+09$ | $2.20E+09$ | $2.20E+09$ | $2.20E+09$ | $2.20E+09$ |

spaced with the ratio of 30 : 40 : 50 : 70. Three strain-gauge instrumented D bolts with anchors of two types were, respectively, installed to measure the bolt load. The strain gauges were fixed to the surface of the D bolts in the middle of the deformable sections. The strains of the strain gauges were measured using the static strain meter SDB-410C. The strains were gradually stabilized 3-4 months after installation. At this time, the axial load of the bolt with anchors spaced evenly was about 105 kN in the outermost section and about 65 kN in the innermost section, but for the bolt with RSA of 30 : 40 : 50 : 70, they were about 90 kN and 70 kN, respectively. The field test is concordant with the numerical simulation results that RSA with the gradual increase to the outermost section of roadway space provides the axial load of the D bolt comparatively equal.

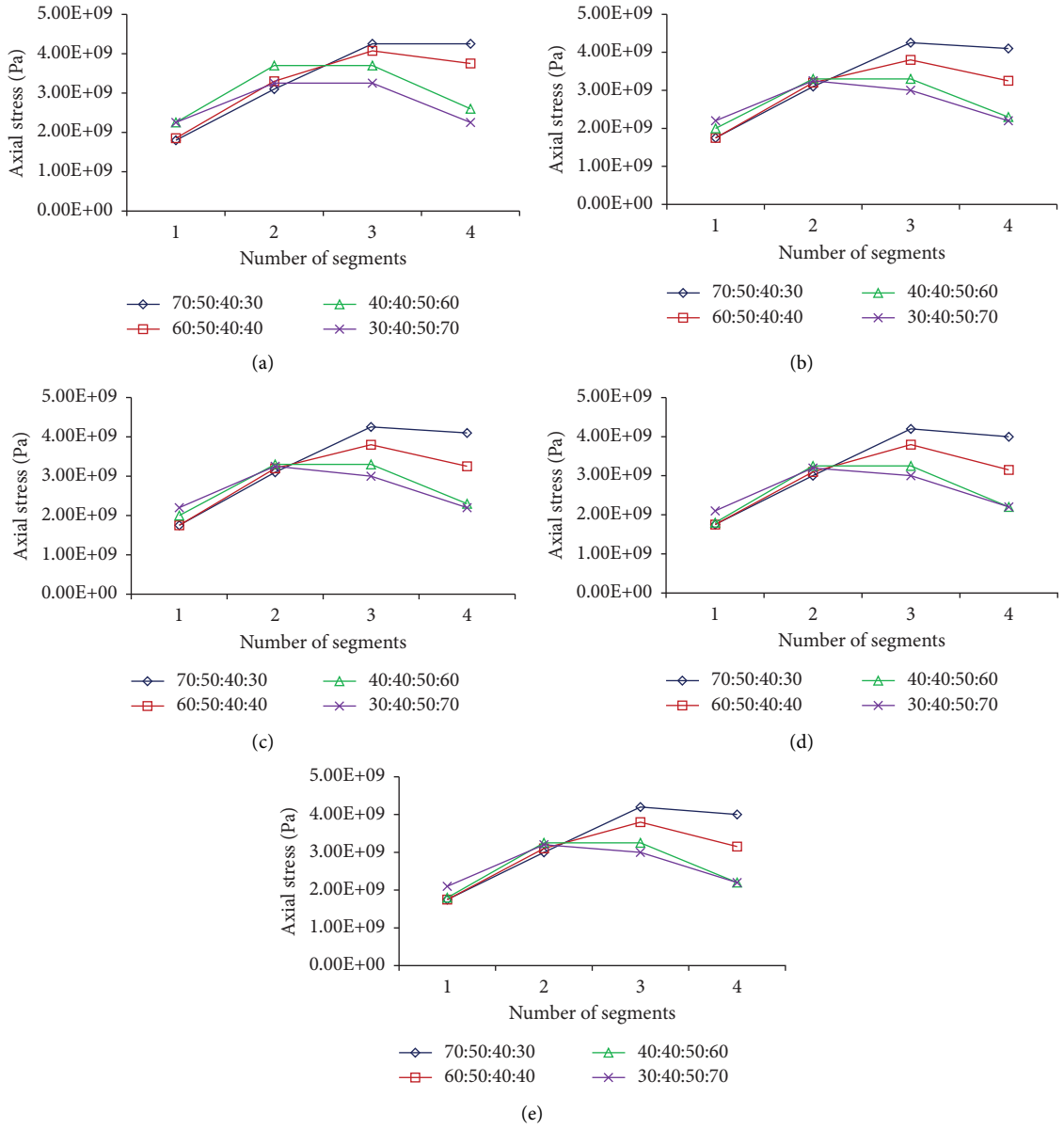


Figure 10: The magnitudes of stresses generated in the deformable sections of D bolts with different ratios of spacing between anchors: (a) the first bolt, (b) the second bolt, (c) the third bolt, (d) the fourth bolt, and (e) the fifth bolt.

## 4. Conclusions

(1) A series of numerical simulations have been conducted to investigate the effects of which D bolt can absorb deformation energy of rock mass around a roadway in comparison with normal fully encapsulated rebar bolt. A methodology for the simulation of D bolt has been proposed to process the numerical analysis. Using this methodology, the displacement of rock mass around a roadway and stress distributions of the bolts can be correctly accessed. Furthermore, the effects of the spacing arrangement of D bolt's anchors on the stress distribution of the bolt can be effectively simulated.

(2) Based on the proposed methodology, the displacement at the top of the roadway roof and the stress distributions of the bolts in the fully encapsulated rebar bolts supported model and the D bolt done model are analyzed, respectively. The results indicate that the displacement of 49 mm at the top of the roadway roof in the D bolts supported model is much larger than 30.08 mm in the fully encapsulated rebar bolts supported model so that the former is capable of absorbing potential deformation energy of rock mass around a roadway to tolerate the large deformation of rock in comparison with the latter. It also implies that the latter may be broken because the

maximum tensile stress of 33 GPa generated in it exceeds the yield strength of bolt material, but the stability of the former is comparatively high because its maximum tensile stress is lower about 10 times.

(3) The plan of spacing arrangement of D bolt's anchors has a significant influence on the stress distribution of the bolt. As a result, when the whole length of D bolt is 2.4 m and the length of its exposed section is 0.1 m, and the number of anchors with the length of 0.1 m is 4, the maximum tensile stress of 3.25 GPa generated in the bolt with RSA of 30 : 40 : 50 : 70 is about 1.13–1.31 times lower than the other D bolts with different ratios of spacing, and the changing range of stress is also the smallest. Therefore, from the viewpoint of supporting a roadway, it is reasonable to employ the D bolt with RSA of 30 : 40 : 50 : 70 so as to provide a comparatively even distribution of stress along its all length. For the given D bolts, RSA of 30 : 40 : 50 : 70 could be provided by setting lengths of their deformable sections as 30 cm, 40 cm, 50 cm, and 70 cm by turns from the innermost section of rock mass around the roadway to the outermost section of roadway space. The result of numerical simulation shows that the selection of spacing between anchors, a main structural parameter of D bolt, has a great significance in preventing its premature failure and improving its load-bearing and deformation capacity.

However, it should be noted that the present study has only considered one arch roadway excavated in a single material subjected to a hydrostatic state of stress. Further studies should be made to investigate the effects of the structural parameters of D bolt associated with various in situ states of stress, opening shapes, and material properties.

## Data Availability

The data used to support the findings of this study are available from the corresponding author upon request.

## Conflicts of Interest

The authors declare that they have no conflicts of interest.

## Acknowledgments

This study was financially supported by the Scientific and Technological Advance of DPR Korea (Grant no. 24-2022-700414).

## References

[1] E. Hoek, P. K. Kaiser, and W. F. Bawden, *Support of Underground Excavation in Hardrock*, CRC Press, Boca Raton, FL, USA, 1995.

[2] C. Li, "A new energy-absorbing bolt for rock support in high stress rock masses," *International Journal of Rock Mechanics and Mining Sciences*, vol. 47, no. 3, pp. 396–404, 2010.

[3] D. Q. Li, Y. C. Li, and W. C. Zhu, "Analytical modelling of load–displacement performance of cable bolts incorporating cracking propagation," *Rock Mechanics and Rock Engineering*, vol. 53, no. 8, pp. 3471–3483, 2020.

[4] D. Q. Li, Y. C. Li, M. Asadizadeh, H. Masoumi, P. C. Hagan, and S. Saydam, "Assessing the mechanical performance of different cable bolts based on design of experiments techniques and analysis of variance," *International Journal of Rock Mechanics and Mining Sciences*, vol. 130, no. 5, Article ID 104307, 2020.

[5] C. C. Li, "A practical problem with threaded rebar bolts in reinforcing largely deformed rock masses," *Rock Mechanics and Rock Engineering*, vol. 40, no. 5, pp. 519–524, 2007.

[6] W. D. Ortlepp, "Yieldable rock bolts for shock loading and grouted bolts for faster rock stabilization," *Mines Magazine of Colorado School of Mines*, vol. 60, no. 3, pp. 12–17, 1970.

[7] D. Q. Li, S. Q. Ma, M. Lane, P. Chang, B. Crompton, and S. A. Hagen, "Laboratory investigations into the failure mechanisms of new yielding and inflatable rockbolts under axial and shearing loading conditions," *Rock Mechanics and Rock Engineering*, vol. 56, no. 1, pp. 565–587, 2023.

[8] W. D. Ortlepp, "The design of support for the containment of rockburst damage in tunnels -an engineering approach," in *Rock Support in Mining and Underground Construction*, P. K. Kaiser and D. R. McCreath, Eds., pp. 593–609, CRC Press, Rotterdam, Netherlands, 1992.

[9] R. Varden, R. Lachenicht, J. R. Player, A. G. Thompson, and E. Villaescusa, "Development and implementation of the Garford dynamic bolt at the kanowna belle mine," in *Proceedings of the 10th Underground Operators Conference, Launceston, AusIMM*, pp. 95–104, Melborune, Australia, April, 2008.

[10] F. Charette and M. Plouffe, "A new rock bolt concept for underground excavations under high stress conditions," in *Proceedings of the Sixth International Symposium on Ground Support in Mining and Civil Engineering Construction, SAIMM*, pp. 225–240, Johannesburg, South Africa, March, 2008.

[11] G. Wang, X. Z. Wu, Y. J. Jiang, N. Huang, and S. G. Wang, "Quasi-static laboratory testing of a new rock bolt for energy-absorbing applications," *Tunnelling and Underground Space Technology*, vol. 38, pp. 122–128, 2013.

[12] A. Ansell, "Dynamic testing of steel for a new type of energy absorbing rock bolt," *Journal of Constructional Steel Research*, vol. 62, no. 5, pp. 501–512, 2006.

[13] A. F. Jager, "Two new support units for the control of rockburst damage," in *Rock Support in Mining and Underground Construction*, P. K. Kaiser and D. R. McCreath, Eds., pp. 621–631, CRC Press, Rotterdam, Netherlands, 1992.

[14] L. St-Pierre, F. P. Hassani, P. H. Radziszewski, and J. Ouellet, "Development of a dynamic model for a cone bolt," *International Journal of Rock Mechanics and Mining Sciences*, vol. 46, no. 1, pp. 107–114, 2009.

[15] M. Cai, "Principles of rock support in burst-prone ground," *Tunnelling and Underground Space Technology*, vol. 36, pp. 46–56, 2013.

[16] B. Simser, W. C. Joughin, and W. D. Ortlepp, "The performance of Brunswick mine's rockburst support system during a severe seismic episode," *Journal of the South African Institute of Mining and Metallurgy*, pp. 217–233, 2002.

[17] M. C. He, W. L. Gong, J. Wang et al., "Development of a novel energy-absorbing bolt with extraordinarily large elongation and constant resistance," *International Journal of Rock Mechanics and Mining Sciences*, vol. 67, pp. 29–42, 2014.

[18] T. Funatsu, T. Hoshino, H. Sawae, and N. Shimizu, "Numerical analysis to better understand the mechanism of the effects of ground supports and reinforcements on the stability of tunnels using the distinct element method," *Tunnelling and Underground Space Technology*, vol. 23, no. 5, pp. 561–573, 2008.

[19] H. W. Jing, Y. H. Li, G. A. Xu, and K. F. Chen, "Analysis of displacement of broken surrounding rock of deep roadway," *Journal of China University of Mining and Technology*, vol. 35, no. 5, pp. 565–570, 2006.

[20] R. Goel, A. Swarup, and P. R. Sheorey, "Bolt length requirement in underground openings," *International Journal of Rock Mechanics and Mining Sciences*, vol. 44, no. 5, pp. 802–811, 2007.

[21] M. S. Muya, B. He, J. T. Wang, and G. C. Li, "Effects of rock bolting on stress distribution around tunnel using the elastoplastic model," *Journal of China University of Geosciences*, vol. 17, no. 4, pp. 337–354, 2006.

[22] Z. S. Du, B. T. Qin, and F. C. Tian, "Numerical analysis of the effects of rock bolts on stress redistribution around a roadway," *International Journal of Mining Science and Technology*, vol. 26, no. 6, pp. 975–980, 2016.

[23] H. Lin, Z. Y. Xiong, T. Y. Liu, R. H. Cao, and P. Cao, "Numerical simulations of the effect of bolt inclination on the shear strength of rock joints," *International Journal of Rock Mechanics and Mining Sciences*, vol. 66, pp. 49–56, 2014.

[24] H. Yu, Z. Y. Niu, L. G. Kong, C. C. Hao, and P. Cao, "Mechanism and technology study of collaborative support with long and short bolts in large-deformation roadways," *International Journal of Mining Science and Technology*, vol. 25, no. 4, pp. 587–593, 2015.

[25] S. Ram, D. Kumar, A. K. Singh, A. Kumar, and R. Singh, "Field and numerical modelling studies for an efficient placement of roof bolts as breaker line support," *International Journal of Rock Mechanics and Mining Sciences*, vol. 93, pp. 152–162, 2017.